

Surface Extensions of 3T3 Cells towards Distant Infrared Light Sources

Guenter Albrecht-Buehler

Department of Cell, Molecular and Structural Biology, Northwestern University Medical School, Chicago, Illinois 60611

Abstract. Using a specially designed phase-contrast light microscope with an infrared spot illuminator we found that ~25% of 3T3 cells were able to extend pseudopodia towards single microscopic infrared light sources nearby. If the cells were offered a pair of such light sources next to each other, 47% of the cells extended towards them. In the latter case 30% of the responding cells extended separate pseudopodia towards

each individual light source of a pair. The strongest responses were observed if the infrared light sources emitted light of wavelengths in the range of 800–900 nm intermittently at rates of 30–60 pulses per min. The temperature increases of the irradiated spots can be shown to be negligible. The results suggest that the cells are able to sense specific infrared wavelengths and to determine the direction of individual sources.

IN previous articles (1, 2) we have presented our rationale for the conjecture that mammalian cells are able to locate infrared light sources at a distance. Therefore, we constructed a special infrared spot-irradiation phase-contrast microscope which presented the cells with microscopically small infrared light sources in their vicinity. Subsequently, we tested the ability of 3T3 cells to produce surface projections which aimed for these sources from a distance.

During the heuristic phase of the project, it became quite clear that the proximity of infrared sources would not simply override all other endogenous and exogenous factors which may contribute to cellular extensions. Therefore, many of the assays that we tried yielded ambiguous results. Still, after more than 800 single cell observations two assays emerged that we consider as acceptable tests for the cells' ability to respond to infrared radiation in a directional manner. The present article reports the results of a subsequent series of separate experiments using only these two assays.

Materials and Methods

Cell Culture

Swiss 3T3 cells were maintained in culture in DME (Gibco Laboratories, Grand Island, NY) supplemented with 10% calf serum and 100 IU of penicillin and streptomycin. Cell cultures were passaged using 0.2% trypsin and 0.2% EDTA in PBS up to the 25th passage. All cells were incubated at 37°C in an atmosphere of 10% CO₂ in air at saturated humidity.

Observation Chamber

The observation chamber had to be very thin to minimize the infrared absorption in the chamber medium and/or to reduce the astigmatism generated by the passage of visible light through the chamber. Therefore, we modified a Dvorak-Stotler Chamber (Nicholson Precision Instruments, Inc., Gaithersburg, MD) by replacing its normally 1-mm-thick stainless steel spacer with a single 50–100- μ m thick Teflon seal (Fig. 1, s).

The Infrared Spot-irradiation Phase-Contrast (IRSIP) Light Microscope

PHASE CONTRAST ILLUMINATOR

Design. The opaque center of the illumination annulus of commercial phase-contrast condensers would have blocked the incident infrared light beam. Furthermore, its glass lenses would have absorbed infrared light above wavelengths of $\lambda > 2.5 \mu\text{m}$ (10). Therefore, we replaced the phase-contrast condenser with a fiber optical illuminator in the shape of a ring (Fig. 1, 4); 5-cm ring diameter, 210 W Intralux, 6,000 illuminator (Volpi, AG, Schlieren, Switzerland) at such a distance below the microscope stage that the objective lens (Fig. 1, 2) imaged it onto its phase ring (Fig. 1, 5). In this way it was guaranteed that all the undiffracted light from the light source passed through the phase ring while the optical axis of the illuminator remained empty for the infrared light to pass freely along its length (Fig. 1, 6). A sapphire lens (5-mm diam; 5-mm focal length; Melles Griot, Rochester, NY) focused the infrared light into the chamber. Sapphire (Al₂O₃) was used because it transmits infrared light up to a wavelength of $\lambda = 7 \mu\text{m}$ (11). To allow the light from the ring illuminator to pass, the sapphire lens was mounted in a transparent Plexiglass plate (Fig. 1, 3).

Field Illumination Wavelengths. Based on our earlier investigations about the least perturbing field illumination spectrum for long-term observation of 3T3 cells (12), in most of the experiments we restricted the light for phase-contrast illumination to a small window between 600 and 700 nm by combining a heatfilter (BG38; Zeiss, Oberkochen, Germany) with a filter (RG 630; Corning Glass Division, Park Ridge, IL). In a special set of experiments (see Results) we used light of 510–560-nm wavelength (peak at 540 nm) by combining a 540-nm interference filter with a CS3-70 absorption filter. All experiments were carried out in a darkened room to avoid effects of other wavelengths contained in the room light.

Intensity. Using a cadmium sulfide photoconductive element as photometer and a Dewar flask filled with 400 ml of distilled water as a calorimeter we determined the normal illumination intensity in the range of wavelengths below $\lambda = 2,000 \text{ nm}$ to be $I = 0.48 \text{ mW/cm}^2$. This intensity is $\sim 1/170^{\text{th}}$ of the total solar irradiance of 80 mW/cm^2 at sea level (11).

THE SPOT ILLUMINATOR

Monochromator. The Beckman monochromator of a dismantled spectrophotometer (model 252; Gilford Instruments, Oberlin, OH) with a 20 W/6V halogen lamp (No. 778; General Electric, Co., Cleveland, OH) served as its infrared light source. Its spectral resolution at our normal set-

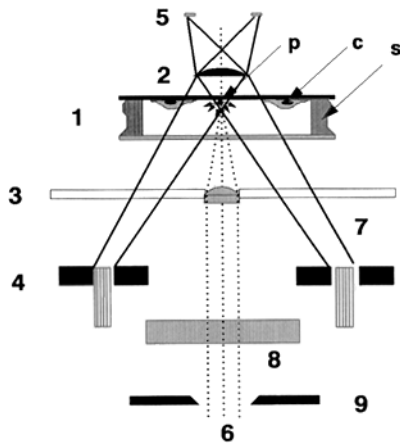


Figure 1. Design of a special phase-contrast condenser with an unobstructed axis for the infrared light beam. The light from a fiber optics ring is focused by the objective lens onto the phase ring. 1, observation chamber (*c*, cell; *p*, infrared light scattering particle; *s*, thin Teflon spacer); 2, objective lens; 3, Plexiglass holder with sapphire lens; 4, fiber optics ring illuminator which emits light in a wide range of directions. The light emitted towards the objective lens (7) is focused by the objective lens onto its phase ring (5). 6, illumination aperture for the infrared light (opening diameter, 100 μm); 8, intensity modulator (see Fig. 2); 9, spot illumination aperture.

ting of the slit width = 1 mm was better than 10 nm as measured with a 3.5 mW HeNe Laser (Metrologic Instruments, Bellmawr, NJ) which emits light at 633 ± 1 nm.

Spot Size. To generate a well-defined outline of the irradiating spot, the light from the monochromator was sent through a small aperture (Fig. 1, 9) which was located 135 mm away from the sapphire lens which imaged it into the observation chamber (Fig. 1, *p*). The aperture was a standard platinum aperture of 100- μm diam used in scanning electron microscopes (E.F. Fullam, Inc., Latham, NY). Its image (= spot size) had a diameter of 3.7 μm , corresponding to a spot area of $A_s = 11 \mu\text{m}^2$. The glare generated by the gain control of the video camera made it appear larger on video images.

Spot Temperature. Estimates show that the infrared light could not raise the temperature of the irradiated spot by more than 0.00001°C (see Appendix).

Incident Infrared Light Intensity. We used a charge-coupled device from a digitizing camera (EDC-1,000; Electric Corp., Princeton, NJ) to compare the intensity of the infrared light spot with the field illumination of the phase-contrast image at wavelengths of 600–700 nm. We found that the spot intensity I_s was approximately three times higher than the normal background, i.e., $I_s = 1.5 \text{ mW/cm}^2$ or $\sim 1/50^{\text{th}}$ of the intensity of sunlight.

INTENSITY MODULATOR

(a) Single Beam Modulator. The early experiments gave the impression that the cells responded much less frequently if the intensity of the infrared radiation remained constant. Therefore, we placed an intensity modulator in the path of the infrared light (Fig. 1, 8; and Fig. 2). It consisted of a rotating disk with a 17-cm diam (Fig. 2 *a*, 1) which intercepted periodically the infrared light beam (Fig. 2 *a*, 4). The disk was rotated by an electric motor at variable rotational speeds of up to 50 rpm.

(i) Rectangular Pulses. If the disk was opaque with 1–4 cut-out sectors we generated 1–4 rectangular on-off pulses of infrared light per revolution. A particular advantage of this modulator was the absence of any additional optical elements through which the infrared light had to pass.

(ii) Sinus-Shaped Pulses. If the disk consisted of polarizing filter material (Fig. 2 *a*, 1) (Edmund Scientific, Barrington, NJ) we generated two sinus-shaped amplitude variations per revolution, provided the infrared light was first polarized by passing through a fixed polarization filter (Fig. 2 *a*, 2). In this case the infrared light had to pass through two polarization filters which reduced its intensity by >75%.

(b) Double Beam Modulator. To generate two side-by-side light spots we replaced the fixed polarizer (Fig. 2 *a*, 2) with a 7-mm-thick plate of a

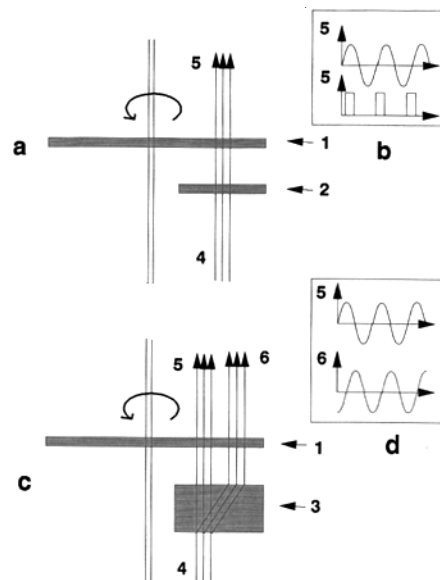


Figure 2. Intensity modulator to generate pulsating infrared light. *a* and *b*, single-beam modulator. The incident infrared light (4) passes through a fixed polarization filter (2) and a rotating polarization filter or masking disk (1) thus generating a sinusoidally or rectangularly changing light amplitude (5) as illustrated in *b*. *c* and *d*, double-beam modulator. A calcite crystal (3) is put in place of the fixed polarizer (*a*, 2), thus generating two sinusoidally alternating light beams (5 and 6) which are shifted in phase by 90° as illustrated in *d*.

calcite crystal (Fig. 2 *b*, 3) over the spot illumination aperture. The crystal consisted of the clear form of Calcite (CaCO_3) which is called “Iceland spar” and transmits infrared light up to 5.5- μm wavelength (11). The birefringence of the crystal produced two images of the aperture (Fig. 2 *b*, 5 and 6) separated by 35 μm whose light was polarized orthogonally to each other. Consequently, the rotating polarization filter modulated the amplitude of the two images in a sinusoidal fashion. Similar to the sinus modulator the double-beam modulator sent the infrared light through several optical elements that reduced its intensity.

SCATTERED INFRARED LIGHT INTENSITY

(a) Tail Irradiation. According to the above estimates, the total incident light power of the spot was $P_i = A_s I_s = 170 \text{ pW}$. At 800-nm wavelength the intensity of the spot as seen with the CCD camera did not decrease noticeably if it passed through a cell, although it was refracted. Therefore, we estimate that the total scattered and absorbed light power P_{sc} was <1%, or $\sim P_{sc} = 2 \text{ pW}$.

(b) Particle Irradiation. To determine the scattering cross-section of the 3.22- μm latex particles (Polysciences Inc., Warrington, PA) at $\lambda = 800 \text{ nm}$ we used a Spektralphotometer (PM6; Zeiss) and a suspension of 11,000 particles/ mm^3 . We found a scattering cross-section of 4 μm^2 , or about half their actual cross-section. Assuming isotropic scattering, one can estimate that the neighboring target cells at an average distance of 35 μm were exposed to a scattering intensity of the infrared light of $I_{sc} = 0.5 \mu\text{W/cm}^2$ which corresponds to $\sim 1/800^{\text{th}}$ of the incident intensity at the location of the particle.

(c) Temperature Control. Considering that the black-body radiation links temperature with infrared light radiation, it was vitally important to maintain a constant and known temperature of the test cells in the observation chamber. Using three stages of control we maintained $37.0 \pm 0.1^\circ\text{C}$ in the following way: (a) Before and during the mounting of the test cells the chamber was kept at 37°C on a warm plate; (b) for the fine control of temperature, the observation chamber on the microscope stage was almost completely enclosed in a hollow aluminum block whose heating cavity was perfused with 4 l/min of 37°C warm water from a thermostat pump (model F 4291; Haake, Karlsruhe, Germany); and (c) for the crude control of temperature a hot air incubator (model 279; Arenberg Sage Inc., Jamaica Plain, MA) blew 37°C warm air at the microscope stage, the heating block, and the objective lens.

Standard Experimental Conditions

Based on a large number of pilot experiments described in the Results section we defined the standard experimental conditions for the two kinds of assays in the following way.

Tail Irradiation Experiments

CELLS:	
cell line:	Swiss 3T3
passage number:	14–25
days in culture:	1–3
FIELD ILLUMINATION:	
wavelength	600–700 nm
intensity	0.48 mW/cm ²
intensity variation:	constant intensity (50 Hz modulation from power line present)
SPOT IRRADIATION:	
site of irradiation:	base of tail
spot size:	3.7 μ m
wavelength:	600–1,700 nm (600 nm serves as control)
intensity:	1.5 mW/cm ²
intensity variation:	sinusoidal, 30/min
DURATION OF EXPERIMENTS:	1–3 h

Particle Irradiation Experiments. For the particle irradiation experiments we modified the above conditions with the following.

SCATTERING PARTICLES

material:	latex
size:	3.22 μ m
distance:	10–110 μ m (average $36 \pm 18 \mu$ m)
location:	perpendicular to the direction of cell locomotion

SPOT IRRADIATION

site of irradiation:	scattering particle
spot size:	3.7 μ m
wavelength:	600–1,700 nm (600 nm for control)
intensity:	1.5 mW/cm ²
intensity variation:	sinusoidal or rectangular, 60/min (initially 24–60/min)
DURATION OF EXPERIMENTS:	1–3 h (Obviously, the experiment ended whenever a cell had contacted a particle, because it would dislocate and attempt to phagocytose it.)

Video Recording

The cells were observed by video recording techniques using a video camera (WY 1550; Panasonic, Secaucus, NJ) and a time lapse video recorder (VTR 8030; Panasonic) at a time lapse factor of 108 \times . The video input signal was averaged over five frames using an Image Sigma Video Processor (model 1794; Hughes Aircraft, Carlsbad, CA) and displayed on a video monitor (WV 5410; Panasonic).

Criteria of Rating

The criteria for different ratings were chosen with the following goals in mind: (a) They should allow observers with little prior experience in cell motility a simple distinction between the different conceivable motile actions of the test cells; (b) they should clearly set apart the “positive” responses (= 3 ratings) from other conceivable motile actions of the test cells; and (c) only experiments with a 3 rating could be considered as support for the thesis that tissue cells are able to locate distant infrared sources.

Consequently, we report only the percentages of experiments with ratings of 3 in the Results section below.

Tail Irradiation Experiments. We rated the recorded video sequences of the cell behavior according to the following scale:

- 0: tail retraction
- 1: no change within the duration of the experiments
- 2: tail thickening
- 3: extension of one or more lamellipodia along the tail

Particle Irradiation Experiments. The video recordings of the particle irradiation experiments were rated by the following scale:

- 0: cell retraction from particle
- 1: no change within the duration of the experiments
- 2: cell extension in the general direction of the particle
- 3: reaching over to the particle across the distance and approaching it closer than 10 μ m.

In both kinds of experiments the ratings did not include an evaluation of the response time of the cells which ranged between 10 min and 1 h. In particular, the cases of short response times posed a problem for the recording of the initial state of the cell. The careful aiming of the infrared beam could take up to 5 min. In several cases, cells began to extend lamellipodia during this time before the recording could begin. However, we found that most of the cells that responded at all began to initiate extensions \sim 20 min after exposure to the infrared light.

Results

Assay 1: Inversion of Cell Polarity after Tail Irradiation

Rationale. It is well established that migrating fibroblasts such as 3T3 cells express morphological polarity by extending ruffling lamellipodia at their leading edge while shaping the trailing portion of their body into a pointed tail. As they extend their leading lamellipodia and slide forward, the tail usually stretches under increasing tension and retracts periodically as one of the phases of the normal locomotory cycle (6). Therefore, it would be the most dramatic change of polarity, if migrating fibroblasts such as 3T3 cells extended large lamellipodia towards their rear. Assay 1 was designed as a test for the possibility to induce such changes by infrared spot irradiation.

Control Levels. We observed 83 individual cells for 1 h or longer in the infrared spot-irradiation phase-contrast microscope without using any infrared spot irradiation. We found that only three cells ($4 \pm 2\%$) extended small lamellipodia at their tails. All others retracted the tail or kept it unchanged during the period of observation.

Infrared Irradiation Experiments. In contrast, we found up to six times as many cells (24%; $p < 0.001$ by t test) extending large lamellipodia towards the rear, if the base of their tail was exposed for 60 min to infrared spot irradiation with a sinusoidally oscillating amplitude at a frequency of 30/min. Fig. 3 shows an example of this inversion of cell polarity in the direction of an infrared spot-irradiated tail of a 3T3 cell. The action spectrum for this response (Fig. 4) was determined on the basis of 29–36 individual cell observations per selected wavelength. It showed a peak around 900 nm.

The decrease of the percentages of responding cells at wavelengths >900 nm may be related to the rise of the absorption coefficient of water in this range of wavelengths. For example, the absorption of water at $\lambda = 1,500$ nm is 200-fold larger than at $\lambda = 900$ nm (11). As a consequence, the incident and scattered light of 1,200-nm wavelength may be too much attenuated by water absorption to provide a sufficiently specific signal to the cells.

The results suggest that the cells were able to redirect their polarity towards the infrared spot source as seen from the cytocenter. However, since they invariably extended the lamellipodia beyond the location of the source, they appeared unable to determine properly its distance.



Figure 3. Extension of a lamellipodium along the tail of a 3T3 cell within 116 min (*arrows, lower panel*) following irradiation of the base of the tail with a spot of infrared light at 900 nm (*upper panel*), that suggests inversion of cell polarity. The location of the irradiation spot is indicated by a circle in each panel. Bar, 30 μ m.

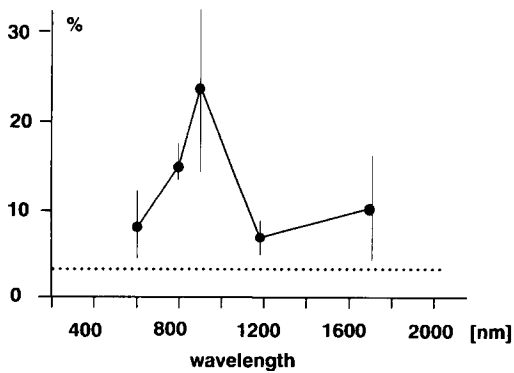


Figure 4. Percentages of cells extending lamellipodia along their tail in response to infrared irradiation of the base of the tail as a function of wavelengths. The dotted line indicated the control-percentage of cells expressing lamellipodia at their tail while the infrared light source was turned off.

Assay 2: Extension of Pseudopodia of 3T3 Cells towards Distant Infrared Light Scattering Objects

Rationale. Assay 2 was designed to test directly the ability of cells to extend a new lamellipodium towards distant sources of infrared light. To generate the required microscopic infrared light sources we deposited latex particles ($3.22 \mu\text{m}$) on the substrate. By aiming the spot illuminator at a particle, we turned it into a pointlike source of scattered infrared light located at approximately the same level as the test cells. To ensure that the test cells were unlikely to approach this light source in the course of their normal locomotion, we selected particle locations at the side of the test cells and $\sim 10\text{--}100 \mu\text{m}$ away from them.

Control Levels. As control experiments we observed cells and particles at similar relative distances and under the standard conditions except that the infrared spot irradiator was turned off. In a series of 57 experiments we observed four cells ($7 \pm 4\%$) which extended lamellipodia towards a particle that was not illuminated by the spot irradiator.

Infrared Irradiation Experiments. After irradiating the particles with infrared light of variable intensity we found that the cells were able to aim new surface projections directly at the light-scattering particles and to contact them (Fig. 5. Please note that we took the photographs in the “off” phase of the intensity modulator whenever possible to improve the visibility of the light-scattering particles). We carried out 160 experiments at a fixed wavelength of 800 nm with 60/min rectangular or sinusoidal variations of the irradiation amplitude and found 32 cases of 3 ratings ($20 \pm 4\%$). The percentage of responding cells could be increased to 47% if we placed a pair of light sources next to each other near the cells (see below). The results are significant at the level of $p < 0.02$ if related by a t test to the above control experiments that used 600–700 nm light for the field illumination. However, as suggested by the action spectrum (see next section) a more appropriate control experiment may use 540 nm light for the field illumination. In this case the results were significant at levels of $p < 0.001$.

Occasionally, a cell aiming for the light-scattering particle extended additional surface projections in other directions. In some of these cases it was obvious that the cell merely continued to extend parts of its leading edge. In other cases the directions of the extensions seemed compatible with Bray’s remarkable observation that cells are able to produce surface extensions that restore the balance of mechanical forces on the cell body (4). The extensions towards the light-scattering particle alone might have unsettled the balance of mechanical forces on the cell, and the additional extensions were needed to restore it.

To determine the action spectrum we irradiated the particles with infrared light of different wavelengths that changed its amplitude 60 times/min in a sinusoidal fashion. We observed between 26 and 160 cells for each wavelength and found again the strongest response around 800 and 900 nm (26 experiments; $23 \pm 9\%$ 3 ratings) compared to the control wavelengths at 600 nm (26 experiments; $8 \pm 5\%$ 3 ratings), 1,200 nm (27 experiments; $4 \pm 4\%$ 3 ratings), and 1,700 nm (30 experiments; $13 \pm 7\%$ 3 ratings) which showed reduced responses (Fig. 6).

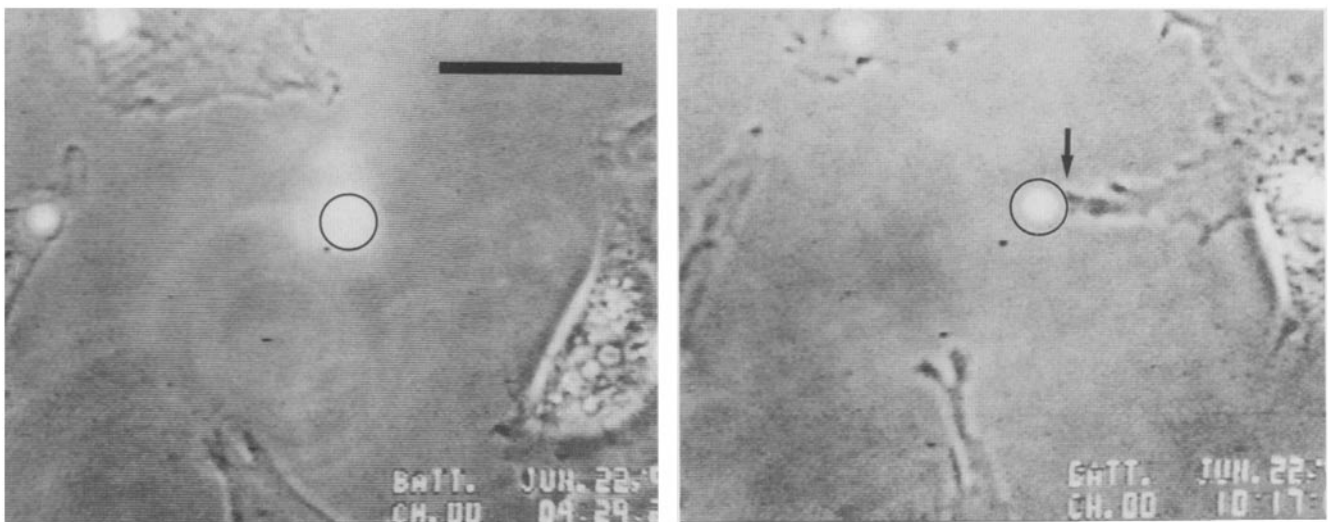


Figure 5. Extension of a separate lamellipodium (arrow, right panel) towards a latex particle that scattered infrared light of 800 nm wavelength for 50 min. The irradiated particle is marked with a circle. The glare in the left hand panel is the result of automatic video gain control during the “on” phase of the spot irradiator. Bar, $30 \mu\text{m}$.

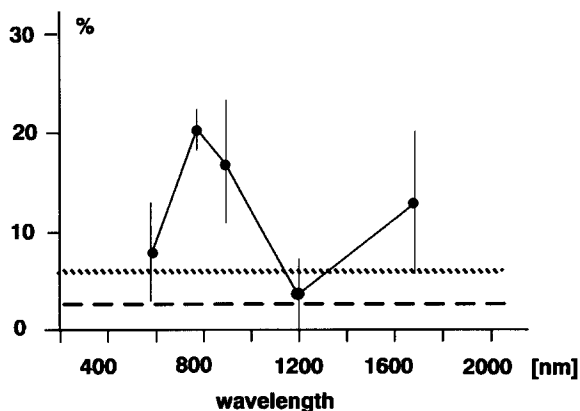


Figure 6. Percentage of cells extending surface projections towards light-scattering latex particles nearby as a function of wavelength. The dotted line indicated the control percentage of cells extending to nearby particles illuminated by field illumination wavelengths of 600–700 nm while the infrared light source was turned off. The dashed line indicates a similar control using a field illumination of 510–560 nm wavelengths.

As mentioned in the case of the tail irradiation experiments, the decrease of the values of the action spectrum at wavelengths longer than 900 nm is presumably the result of a strong absorption peak of water around 1,500 nm (11).

Field Illumination Control. The above mentioned control levels of 7% for unirradiated particles were surprisingly high. In view of the value of the action spectrum at 600–700 nm it seemed conceivable that the particles scattered enough of the 600–700 nm light from the field illumination to be detected by the cells. Therefore, we added a further control by changing the wavelength of the field illumination to \sim 510–560 nm (peak at 540 nm) and counting the number of cells that would aim separate surface projections at unirradiated particles nearby. At this wavelength and illumination intensity the cells continued to extend ruffling lamellipodia during several hours of continuous observation. We found two cases of 3 ratings among 59 experiments ($3 \pm 2\%$). If related to this control level, the peak value of the action spectrum is significant on the level of $p < 0.001$.

Distance-Response Curve. To measure the effect of particle distance on the frequency of directed cellular extensions we pooled all experiments with irradiation wavelengths between 800 and 900 nm regardless of rate and shape of the infrared pulses. We sorted the results according to the initial distance between cell edge and particle. The sorting intervals had sizes of $20 \mu\text{m}$ and contained between 51 and 158 experiments each. We found, indeed, that the percentage of responding cells decreased with distance (Fig. 7), although not as steeply as we would have expected on the basis of the decrease of scattered light intensity.

These counts did not reflect that the cells often retracted their pseudopodia after coming closer than 5–10 μm to the particle for which they had apparently aimed. Such retractions did not affect the rating (see definition of rating above), but they suggested that the infrared sources at close range lacked certain properties that the approaching cell seemed to “expect.”

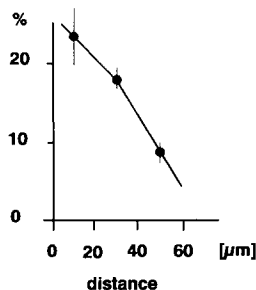


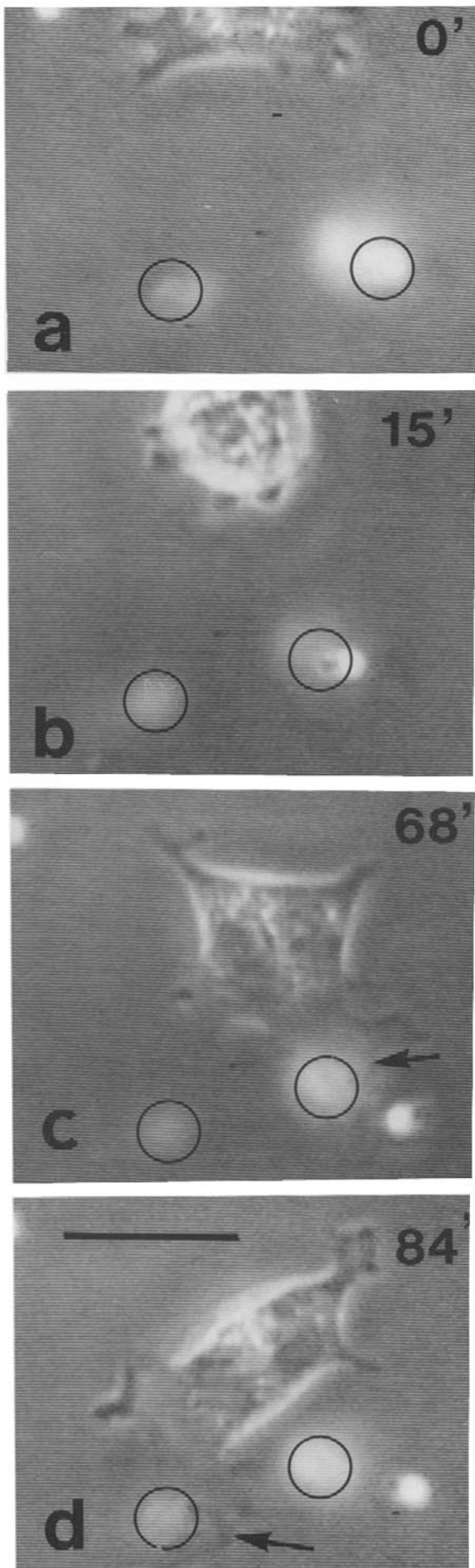
Figure 7. Distance-response curve for cells extending towards infrared light-scattering particles at wavelengths between 800 and 900 nm regardless of pulse frequency and shape. The columns represent the percentage of cells reaching over to a particle that was located away from the nearest cell edge within the indicated limits. The sample size for each column was between 51 and 158 experiments each.

Alternate Cell Responses. Instead of sending extensions directly to the light-scattering particles, several cells appeared to use other methods of approaching them. For example, we observed cells that aimed for a particle right next to the scattering one. Such results received 2 ratings and thus did not contribute to the reported data that reflect only 3 ratings. Yet, they may reveal a certain degree of inaccuracy of the aiming mechanism, or else they may suggest that the approached particle scattered enough secondary light to become a suitable target for the cell. In other cases we observed cells that rounded up completely, and subsequently respread while pointing their new leading lamellipodium towards the particle (e.g., Fig. 8). Yet others migrated in a loop before they headed for the scattering particle. Such cases may suggest the presence of certain cytoskeletal constraints that have to be overcome before the cell can approach a light source.

Distinction between Infrared Phototaxis and Cellular Localization of Surrounding Infrared Light Sources. According to present understanding, phototaxis depends strictly on the total sum of the light intensities at the location of the cellular photoreceptors. Consequently, it cannot determine the number of contributing individual light sources. In contrast, the postulated function of the centrosome as a mapping device for signal sources (1) would be able to distinguish between different signal sources by determining the different angles of incidence.

Experimentally, one may distinguish between these two possibilities by placing two light sources next to each other. If the cell subsequently extends down the middle between them or approaches only one of them, it is likely to detect them by phototaxis. On the other hand, if it aims separate extensions at each source, it is likely to express a mapping ability for the different source locations.

We generated two side-by-side light spots by replacing the fixed polarizer with a birefringent plate of calcite crystal (Fig. 2c) and selected a cell near two particles separated by the appropriate distance. In 41 experiments using 800 nm as irradiation wavelength we found 20 cases ($47 \pm 10\%$) where the cells extended lamellipodia in the direction of the two light sources. The results suggest that the cells responded better to two closely adjacent light sources than to one. Among the responding cells there were six cases ($30 \pm 12\%$) which extended lamellipodia first to one and subsequently to the other light source (Fig. 8), suggesting that they were able to recognize that there were two individual sources. In three



cases the cells seemed to extend to two or more lamellipodia simultaneously towards both light sources (Fig. 9).

The cases where the cells approached first one and then the other light source seem to be particularly significant to exclude phototaxis as the explanation. After the cell reached one of the light sources (e.g., Fig. 8 c) parts of its body were no longer exposed to the scattered light alone, but to the much stronger primary beam. If it were merely phototactic, it seems very unlikely that it would leave the area of highest intensity and follow the scattered radiation of a much weaker second light source as in Fig. 8 d.

Discussion

The results suggest that 3T3 cells ignored particles nearby that scattered light of constant intensity if its wavelength was ~ 540 nm. However, if the color of the scattered light belonged to the range between the far red and near infrared, then a small percentage of the cells seemed to detect the particles at a distance and to aim lamellipodia at them. This percentage increased dramatically to $\sim 25\%$ if the infrared light of 800–900 nm was pulsating and even further to $\sim 47\%$ if two particles were located next to each other. Under these circumstances some cells seemed able to reach over to both light sources individually.

At this very early stage of the investigation it is not possible to identify a biological function for this kind of infrared "vision" of tissue cells. Perhaps it aids them to locate the source of a chemical gradient by detecting altered infrared emissions in the direction of the source. Perhaps it allows them to locate distant others by certain bursts of infrared emissions that these cells emit in the course of their metabolic processes. Obviously, such bursts would not have to be strictly periodic like the light pulses used in our experiments. These and other possibilities will have to be tested in the future.

As pointed out in the Appendix, the observed cellular responses cannot be attributed to temperature effects, because the infrared radiation raised the local temperature by only a negligible amount. Also the reduced response of the tail-irradiated cells at $\lambda = 1,200$ nm excludes the possibility that we are observing temperature effects. Cells contain $\sim 85\%$ water which has a 30 times larger absorption coefficient at 1,200 nm than at 900 nm (11). Consequently the water in the cytoplasm of the irradiated tail region absorbed 30 times more infrared energy at 1,200 nm than at 900 nm. If heating effects would explain the results, one would expect a weaker response at 900 nm than at 1,200 nm, contrary to the results.

The results cannot be explained by chemotactic effects of the latex particles, either, because the cells were not chemotaxing towards unirradiated particles. Therefore, the results suggest that 3T3 cells have the ability to locate and resolve individual infrared light sources at a distance. We are tempted to call it a cellular ability "to see objects" and to consider the results as support for our earlier suggestions that cytoplasm has a certain capacity of data processing and integration (2).

Although the percentage of ~ 25 – 47% responsive cells in

Figure 8. Sequential extension of a 3T3 cell towards two separate light sources of 800 nm. Initially the cell rounded up (b) extended first to one light source while dislodging the latex particle (c), and then to the other (d). Bar, 30 μm .

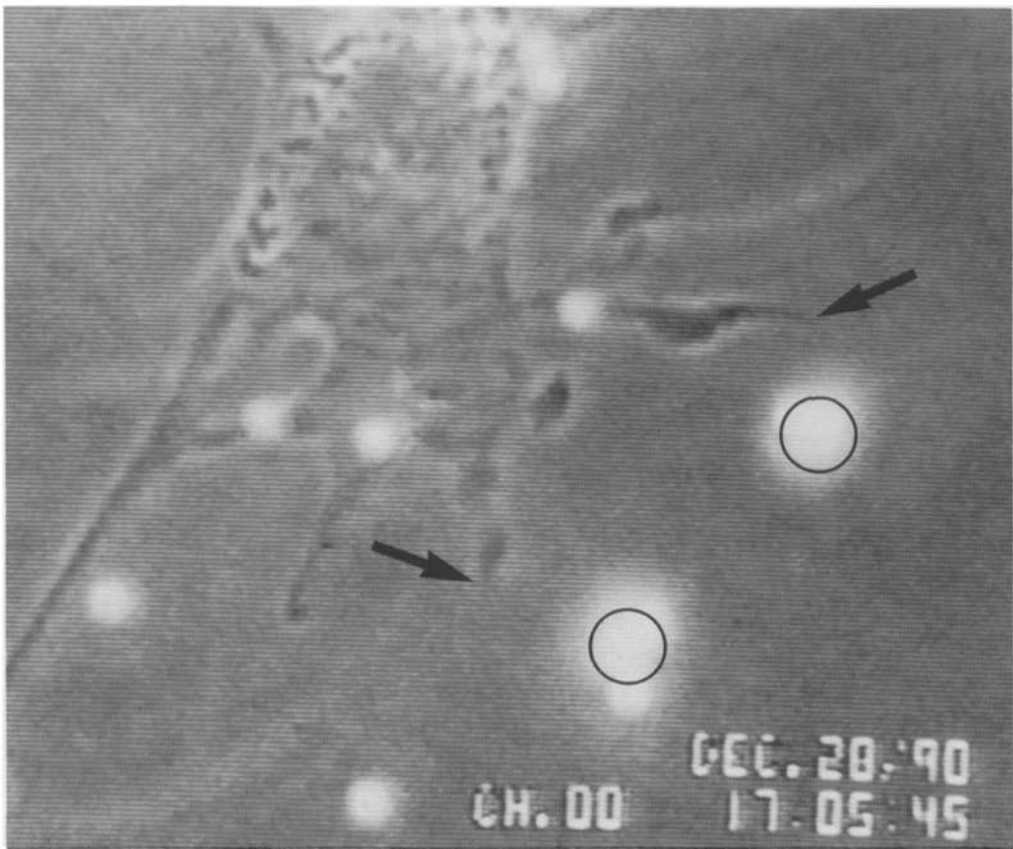
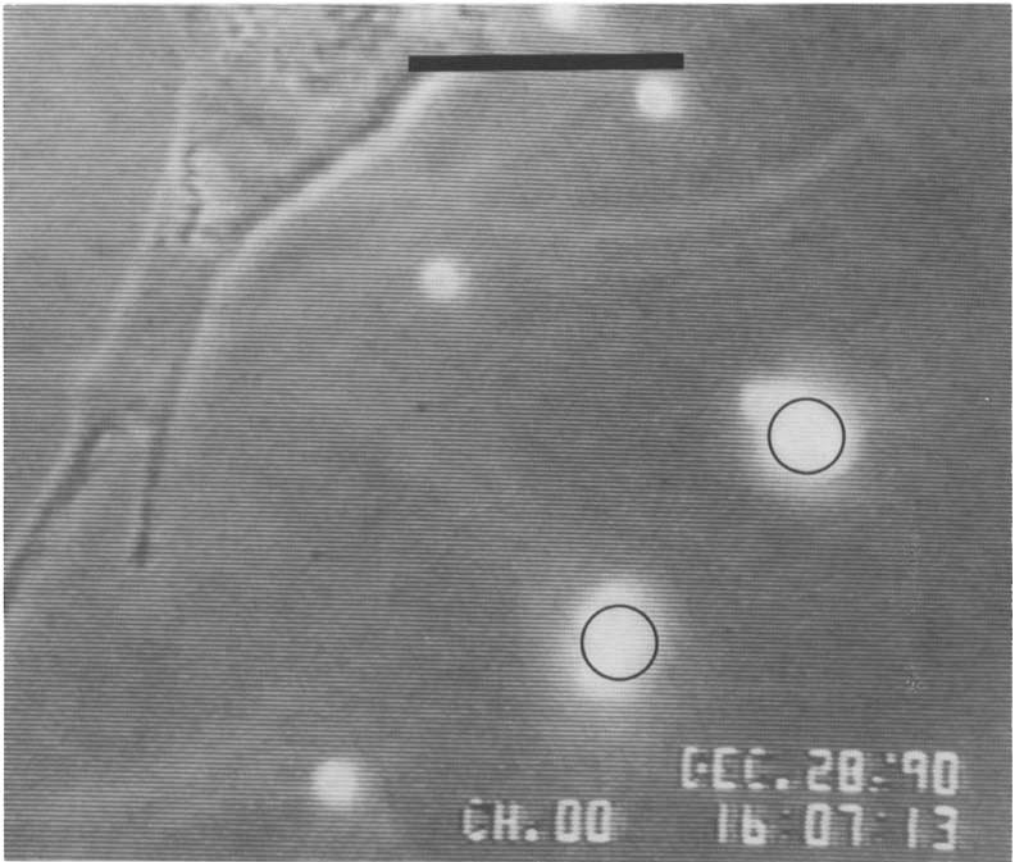


Figure 9. Apparent parallel extensions of a 3T3 cell towards two separate light sources of 800 nm. In the course of 58 min a migrating 3T3 cell extended from its side a large lamellipodium in the direction of the two light sources which frayed into four thinner extensions. Two of the four appeared to approach the light sources (*arrows, lower panel*). Bar, 30 μm .

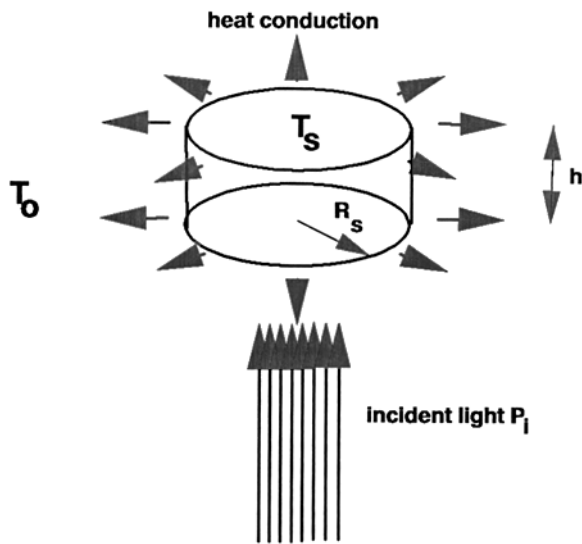


Figure 10. Schematic to estimate the temperature increase at the spot of infrared irradiation (for explanation see text).

our experiments was significantly above control levels, it may appear low, nevertheless. To evaluate the significance of the results, several factors should be taken into account that may affect the response frequency of the cells. For example, since our assays depended on the ability of cells to extend lamellipodia, any factors which reduce cell motility will also reduce the response frequency in our experiments. In particular, cell line, clone, culture age, passage number, and other culture conditions (3) may be important parameters for the assays used. Furthermore, the numerical evaluation of the experiments reflected the responses of the cells in only limited ways. For example, the degree of accuracy in the apparent aiming of the cells (Fig. 5) and the unusual outlines of their surface extensions were not expressed in the percentages of 3 ratings. Finally, if our concept of data processing and signal-integrating cells (2) is correct, then we should not expect that cells respond quantitatively to most environmental signals. It seems more likely, that a mechanism of data integration will consider many different signals and attach different weights to them, thus preventing any particular environmental cue from dominating all the others.

The results point to the existence of cellular receptor pigments that absorb in the spectral range of 800–900 nm. Such pigments have, indeed, been observed. For example, the peak absorption of several kinds of bacterial chlorophyll is located in this range (8). Other pigments are known to absorb far red and infrared light. For example, chlorophyll has its absorption peak at 680 nm (7) whereas the infrared receptors in the facial pits of rattle snakes detect wavelengths in the range of 2–3 μm and larger (5).

We do not know yet how large the cellular receptor area for the infrared radiation may be. Assuming that our earlier speculation is correct about the centrosome as the cellular detection and mapping device (1), the putative receptor area A_r would be as large as the dimensions of two centrioles, i.e., $A_r = 2 * 0.1 * 0.5 \mu\text{m}^2 = 10^{-9} \text{cm}^2$. At an average distance of 35 μm from a particle that scatters infrared light of 900-nm wavelength with an intensity $I_{sc} = 0.5 \mu\text{W}/\text{cm}^2$ the centriole would receive the infrared energy of $E = 5$

$\times 10^{-16} \text{W}$, which corresponds to $\sim 2,500$ photons/s at a wavelength of 900 nm. Considering that retinal cells have been shown to detect single photons of visible light, it appears that our speculation about the role of centrioles in the localization of infrared light sources is at least compatible with the results reported here.

Appendix

Infrared Spot Temperature

The incident infrared light could conceivably raise the temperature of the scattering object. Thus, it must be excluded that the observed effects on the target cells are caused by temperature effects. Therefore, we calculated the local increase in temperature under the "worst case" assumption that all the incident light energy was absorbed by the volume of the scattering object.

Assume that absorption of the incident infrared light power P_i has raised the temperature of the scattering object to the level T_s above the ambient temperature T_0 . As a consequence a temperature gradient forms across the radius R_s of the spot and conducts heat energy away into the surrounding aqueous medium (Fig. 10). The amount of heat conducted per second is

$$\Delta Q = \gamma A (T_s - T_0) / R_s \quad (\text{A1})$$

where A is the total surface area of the cylinder that represents the scattering object in Fig. 10

$$A = 2R_s^2 \pi + 2R_s \pi h, \text{ and} \quad (\text{A2})$$

γ the thermal conductivity of water at 37°C, $\gamma = 6.23 \text{ mW}/\text{cm}^\circ\text{C}$ (9). Under steady-state conditions, the incident heat is equal to the heat conducted away:

$$\Delta Q = P_i. \quad (\text{A3})$$

From Eq. 1, 2, and 3 it follows that

$$T_s - T_0 = P_i R_s / \gamma A \quad (\text{A4}).$$

With $R_s = 1.9 \mu\text{m}$ (radius of the spot), $P_i = 0.2 \text{ nW}$ (incident light power), $h = 3 \mu\text{m}$ (approximate thickness of scattering particle or cell), Eq. 2 yields $A = 58 \times 10^{-8} \text{cm}^2$, and Eq. 4 yields

$$T_s - T_0 = 0.00001^\circ\text{C} \quad (\text{A5}).$$

In reality the temperature increase at the spot can be expected to be even smaller, because the material at the spot absorbs <1% of the incident energy. Therefore, we can safely ignore the possibility that any observed effects on the target cells are because of temperature increases at the point of infrared light irradiation.

I thank Dr. Martin Zand for this critical reading of the manuscript and Mr. Robin Donner for his excellent technical assistance.

Requests for support of this work to the National Institute of Health have consistently received some of the lowest ratings by the Cell Biology Study Sections. Therefore, I am particularly grateful for the unwavering support and personal encouragement by Dr. Igor Vodyanoy from the Office of Naval Research (Grant N0014-89-J-1700) and Dr. Shirley Tove from the United States Army Research Office (Grant ARO 122-89).

Received for publication 7 February 1991 and in revised form 26 March 1991.

References

1. Albrecht-Buehler, G. 1981. Does the geometric design of centrioles imply their function? *Cell Motility*. 1:237–245.
2. Albrecht-Buehler, G. 1985. Is cytoplasm intelligent too? *In Cell and Muscle Motility*. Jerry W. Shay, editor. Vol. 6:1–21.
3. Albrecht-Buehler, G., and R. M. Lancaster. 1976. A quantitative description of the extension and retraction of surface protrusions in spreading 3T3 mouse fibroblasts. *J. Cell Biol.* 71:370–382.
4. Bray, D. 1979. Mechanical tension produced by nerve cells in tissue culture. *J. Cell Sci.* 37:391–410.
5. Bullock, T.H., and G. J. Cowles. 1952. Physiology of an infrared receptor: the facial pit of pit vipers. *Science (Wash. DC)*. 115:541–543.
6. Chen, W. T. 1981. Mechanism of retraction of the trailing edge during fibroblast movement. *J. Cell Biol.* 90:187–200.
7. Darnell, J., H. Lodish, and D. Baltimore. 1990. *Molecular Cell Biology*.

- 2nd edition. W. H. Freeman and Co. New York.
8. Fuller, R. C., S. F. Conti, and D. B. Mellin. 1963. The structure of the photosynthetic apparatus in the green and purple sulfur bacteria. *In* Bacterial Photosynthesis. H. Gest, A. San Pietro, and L. P. Vernon, editors. 71-87. The Antioch Press, Yellow Springs, OH.
 9. Handbook of Chemistry and Physics. 1976. R. Weast, editor. 57th edition. CRC Press, Inc., Boca Raton, FL.
 10. Martin, A. E. 1966. *Infra Red Instrumentation and Techniques*. Elsevier Science Publishing Co. Inc., New York.
 11. Wolfe, W. L., and G. J. Zissis. 1989. *The Infrared Handbook*. 3rd edition. Environmental Research Institute of Michigan.
 12. Zand, M., and G. Albrecht-Buehler. 1989. Long-term observations of cultured cells by interference-reflection microscopy: near-infrared illumination and Y-contrast image processing. *Cell Motil. and the Cytoskeleton*. 13:94-103.